ISSN 0005-1179 (print), ISSN 1608-3032 (online), Automation and Remote Control, 2025, Vol. 86, No. 1, pp. 48–60.

CONTROL IN TECHNICAL SYSTEMS

Hardware-in-the-Loop Simulation of Control System for Vertical Plasma Position in KTM Tokamak

A. E. Konkov[*,a], V. I. Kruzhkov[*,b], E. A. Pavlova[*,c], P. S. Korenev[*,d], B. Zh. Chektybayev[,e], S. V. Kotov[**,f], D. B. Zarva[**,g], and A. A. Zhaksybayeva[**,h]**

[*] *Trapeznikov Institute of Control Sciences, Russian Academy of Sciences, Moscow, Russia*
[**] *The Institute of Atomic Energy of the National Nuclear Center, Kurchatov, Republic of Kazakhstan*
e-mail: [a] konkov@ipu.ru, [b] kruzhkov@ipu.ru, [c] pavlova@physics.msu.ru, [d] pkorenev@ipu.ru, [e] chektybaev@nnc.kz, [f] ksvlondon@mail.ru, [g] zarva@nnc.kz, [h] zhaksybaeva@nnc.kz

Received July 11, 2024
Revised September 13, 2024
Accepted September 20, 2024

Abstract—The article is devoted to the development of a digital control system for the unstable vertical plasma position in the KTM tokamak. A controller with fixed parameters was synthesized using an array of plant models. The synthesized controller ensures the desired control performance and robust stability margins simultaneously for two plant models with varying parameters. A robust stability analysis was carried out. The performance of the system was verified through hardware-in-the-loop (HIL) simulation using a complete nonlinear model of the voltage inverter, taking into account its maximum current and voltage limitations.

Keywords: tokamak, KTM, hardware-in-the-loop simulation, robust controller, LMI

DOI: 10.31857/S0005117925010048

1. INTRODUCTION

Control systems for the vertical plasma position are critically important for the operation of modern D-shaped tokamaks, where the plasma is elongated vertically in the poloidal cross-section [1–4]. The vertical position of the plasma in such tokamaks is inherently unstable, so a feedback control system is employed to provide plasma discharges. The vertical plasma position is controlled via a magnetic field generated by the current in the horizontal field coil (HFC) [5]. The vertical plasma position control system must ensure the stability of the plasma's vertical position and achieve the desired scenario for the vertical plasma position throughout the discharge.

The KTM tokamak (Kazakhstan Tokamak for Material testing) [6, 7] is located in Kurchatov, Kazakhstan. In addition to the HFC, the tokamak uses six poloidal field (PF) coils, a central solenoid (CS) for induction of the plasma current, a toroidal field coil, and a passive stabilization coil for the plasma position. Figure 1 shows the coil arrangement of the KTM tokamak.

The plasma in the tokamak is a non-stationary control plant; in particular, the dynamics of the vertical plasma position can change significantly during a discharge and may vary strongly in discharges with different scenarios. Previously, in [8], models of vertical plasma displacement were calculated for several shots, a control system for the HFC current was synthesized, and estimates of the controllability region for the vertical plasma position were obtained. A new HFC power supply, implemented as a voltage inverter operating in pulse-width modulation (PWM) mode, is planned for commissioning at the KTM tokamak. The goal of this work is to develop and perform hardware-in-the-loop simulation of a digital control system for the vertical plasma position with the new power supply. A static controller is synthesized to provide acceptable control quality and the necessary robust stability margins for the closed-loop control system under two different plasma discharge scenarios.

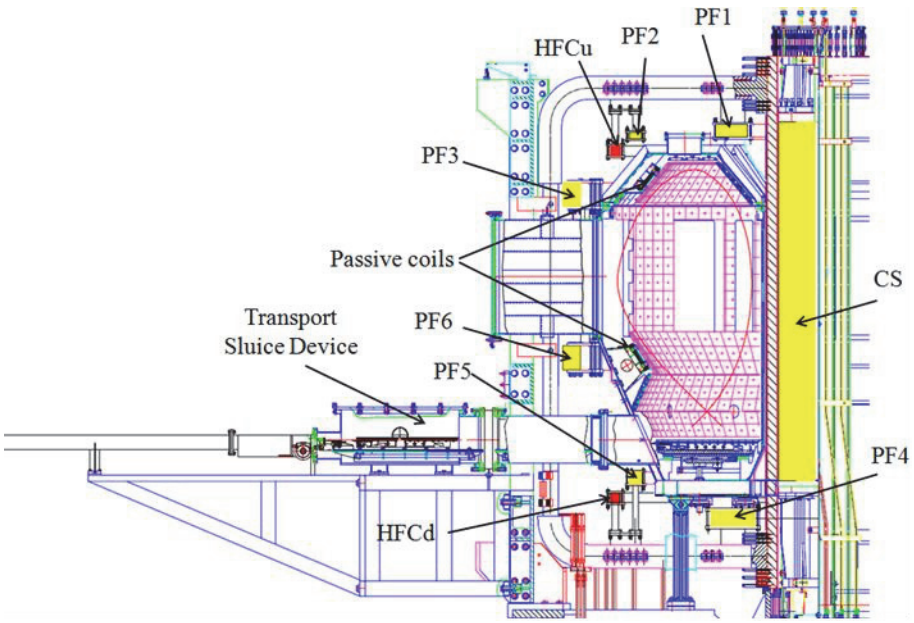

Fig. 1. Cross-section of the KTM tokamak.

Hardware-in-the-loop simulation [9] is an important stage before implementing the developed control system in experimental practice. In this method, the controller operates on real equipment that is functionally identical to what will be used in practice. With sufficiently accurate modeling of the controlled plant, hardware-in-the-loop simulation can guarantee the operability of the developed control system's and reduces implementation costs. This work proposes a methodology for conducting hardware-in-the-loop simulation of a cascade control system for the vertical plasma position and presents its results under various operating modes.

The problem statement, the structural diagram of the synthesized control system, and the description of the plasma models used are provided in Section 2. Section 3 describes the synthesis of the cascade control system for the vertical plasma position. Section 4 presents the analysis of the robust stability margins of the synthesized system in terms of gain and delay. Section 5 includes the results of hardware-in-the-loop simulation of the synthesized control system in normal and extreme operating conditions, enabling the verification of results obtained in Sections 3 and 4. The conclusion summarizes the main findings. The appendix compares the digital control system synthesized directly on the discrete plant model with the discretized system tuned on the continuous model, assuming the same tuning method is used for both, this is the justification for the choice of the control system synthesis method.

2. PROBLEM STATEMENT

The structural scheme of the digital cascade control system for the vertical plasma position in the KTM tokamak is shown in Fig. 2, where Z_{ref} is the reference for the vertical plasma position, Z is the vertical plasma position, $e_Z = Z_{ref} - Z$ is the vertical plasma position error, $I_{HFC\ ref}$ is the reference for the HFC current, I_{HFC} is the HFC current, $e_{I_{HFC}} = I_{HFC\ ref} - I_{HFC}$ is the HFC current error, U_{HFC} is the HFC voltage, and u_{PWM} is the control signal.

The actuator in the control system is a power supply for the HFC, implemented as a voltage inverter operating in PWM mode with the following parameters: three voltage levels $[-1, 0, 1]$ kV; power of 2 MW, corresponding to a maximum current of ± 2 kA; and a PWM frequency of 1 kHz. The voltage inverter consists of an H-bridge and a PWM controller, which converts the control

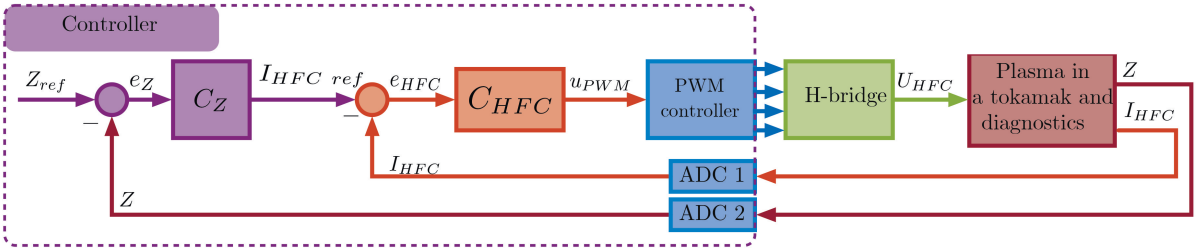

Fig. 2. Block scheme of the digital cascade control system for plasma vertical position in KTM with a voltage inverter in PWM mode.

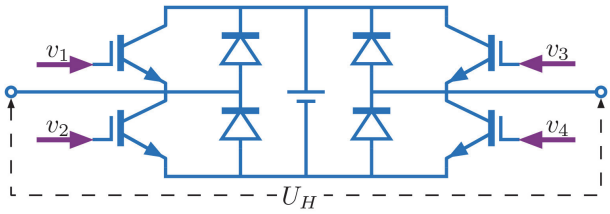

Fig. 3. Schematic diagram of an H-bridge with a DC voltage source.

signal u_{PWM} into pulse sequences v_{1-4} that control the H-bridge transistor gates (Fig. 3). There is no digital-to-analog converter (DAC) in the control system; instead, the PWM controller, as part of the digital control device, directly drives the gates of transistors via optocouplers with its digital outputs v_{1-4}.

The HFC comprises two sections connected in a series-opposing configuration. The voltage and current in the HFC are related by

$$L\dot{I}_{HFC}(t) + RI_{HFC}(t) = U_{HFC}(t),$$

where $R = 212$ mΩ is the HFC resistance, and $L = 17$ mH is the HFC inductance. The discrete transfer function of the HFC is

$$P_{HFC}(z) = \frac{R^{-1}\bigl(1 - \exp(-T_sR/L)\bigr)}{z - \exp(-T_sR/L)}, \quad I_{HFC}(z) = P_{HFC}(z)U_{HFC}(z), \tag{1}$$

where z is the Z-transform variable, and $T_s = 1$ ms is the sampling time.

Models of vertical plasma displacement in the KTM tokamak [8] were obtained from experimental data for two of the most typical plasma shots with a plasma current of 500 kA from the last experimental campaign [10]: shot no. 5121 with an elongation (the ratio of vertical to horizontal plasma diameters) of 1.4 and a normal duration, and shot no. 5126 with an elongation of 1.6 and a short plasma confinement time. These models are represented as linear state-space models with time-varying parameters in discrete time:

$$\begin{cases} x(T_sk + T_s) = A(T_sk)x(T_sk) + B(T_sk)u(T_sk) \\ y(T_sk) = C(T_sk)x(T_sk), \end{cases}$$

where $x = \left[I_{PF}^{\mathrm{T}}\ I_{VV}^{\mathrm{T}}\ I_P\right]^{\mathrm{T}} \in \mathbb{R}^{24\times1}$ is the state vector, $I_{PF} \in \mathbb{R}^{8\times1}$ is the vector of currents in the poloidal field coils (including I_{HFC}), $I_{VV} \in \mathbb{R}^{15\times1}$ are the currents in the vacuum vessel and passive structures, I_P is the plasma current, $u = U_{HFC}$ is the input, and $y = [Z\ I_{HFC}]^{\mathrm{T}}$ is the output vector.

For each vertical plasma displacement model, the set of matrices $\{A, B, C\}$ was calculated with a sampling time of $T_s = 1$ ms:

(1) Model of shot no. 5121 – for 1001 time points from 2.50 to 3.50 s;

(2) Model of shot no. 5126 – for 61 time points from 2.44 to 2.50 s.

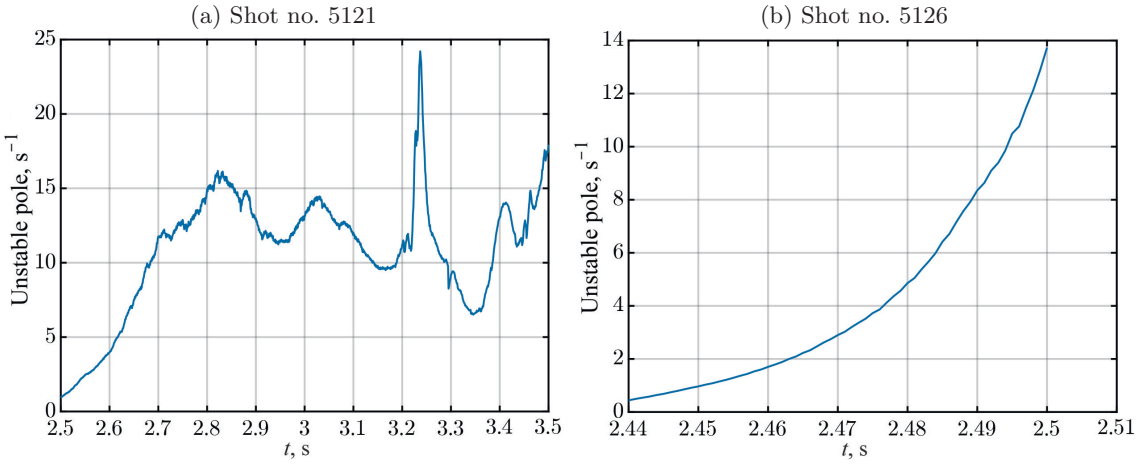

Fig. 4. Change in the magnitude of the single unstable pole of the plasma vertical motion models during the shot.

Both models have one unstable pole that varies significantly during the shot, as shown in Fig. 4. For controller synthesis, an array of discrete transfer functions was computed:

$$P_n(z) = C_n(zI - A_n)^{-1}B_n, \tag{2}$$

where the index n denotes the time point for which the model matrices were calculated: $A_n = A(T_s n)$, $B_n = B(T_s n)$, and $C_n = C(T_s n)$.

The controller must ensure that the control system has the necessary robust stability margin to provide acceptable control quality simultaneously for both vertical plasma displacement models with time-varying parameters. The control system must also have a sufficient phase stability margin to maintain stability when a transport delay of up to 10 ms (10 sampling steps of 1 ms each) is introduced into the feedback loop, which is the upper limit of possible delays in the data acquisition, processing, and transmission system of the KTM tokamak. The delay is modeled by incorporating a discrete transfer function z^{-10} into the feedback loop.

3. CASCADE CONTROL SYSTEM SYNTHESIS

The controllers in both control cascades were synthesized using the method described in [11], which allows for the synthesis of a discrete controller based on a set of discrete plant models and performs loop shaping of the open-loop transfer function. The synthesis is carried out using linear matrix inequalities through a convex-concave procedure. An alternative approach is discussed in the Appendix, where the controller is synthesized based on the continuous-time model of the plant, and then the controller is discretized.

First, the inner current control loop for the HFC is synthesized based on the model (1). The linear model of the voltage inverter was obtained by identifying the serial connection of the HFC and the voltage inverter using the approach described in [12]. As a result, a PI-controller was synthesized with the discrete transfer function

$$C_{HFC}(z) = K_{P_{HFC}} + K_{I_{HFC}}\frac{T_s z}{z-1}, \quad u_{PWM}(z) = C_Z(z)e_{HFC}(z), \tag{3}$$

where $K_{P_{HFC}} = 0.004$ V/A and $K_{I_{HFC}} = 0.15$ V/(A × s). The output of the controller, u_{PWM}, is limited to the range ±1 V, which is determined by the parameters of the PWM controller. The synthesized current control system for the HFC provides the fastest possible performance subject to the limitations of the power supply, which allows the current rise rate in the HFC to reach $U_{\max}/L = 58.8$ kA/s. This control system was used in [8] to estimate the controllability region of the vertical plasma position.

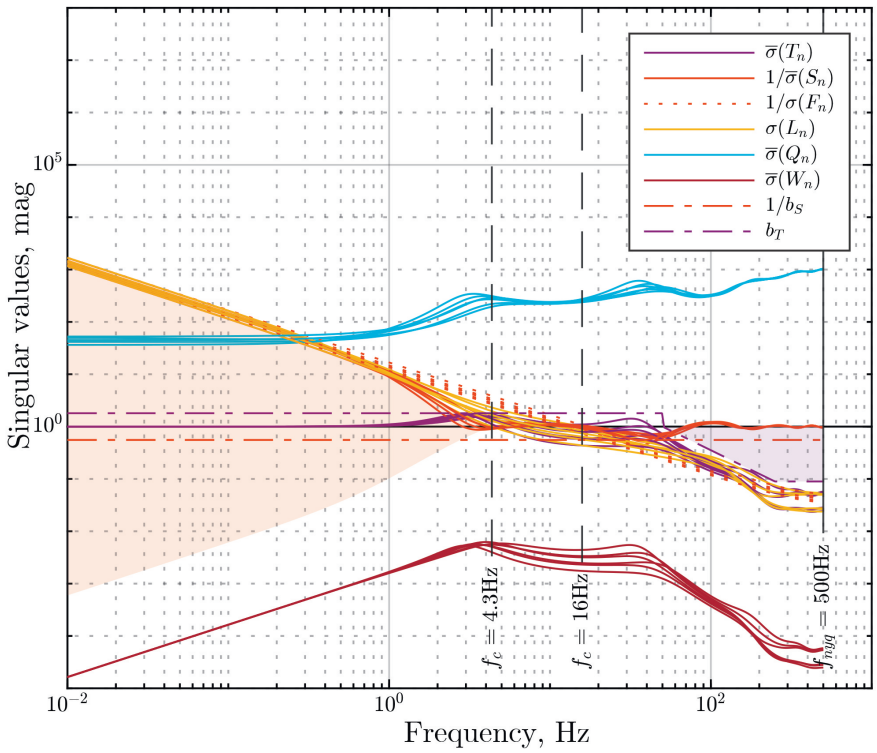

Fig. 5. Bode plot of the transfer functions of the plasma vertical position control system.

The synthesis of the outer control loop was performed on the set of discrete transfer functions of the inner loop: $Z(z) = G_n(z)I_{HFC\ ref}(z)$,

$$G_n(z) = P_n(z)A(z)C_{HFC}(z)\Big(I + P_n(z)A(z)C_{HFC}(z)\Big)^{-1}, \tag{4}$$

where $A(z) = U_{\max} z^{-T_{PWM}/T_s}$ is the linear model of the voltage inverter, $U_{\max} = 1$ kV, $T_{PWM}/T_s = 1$, and n is the index from (2). Thus, one controller will meet the given quality and robust stability criteria simultaneously for both models with variable parameters. As a result, a PID-controller was synthesized with the discrete transfer function

$$C_Z(z) = K_{P_Z} + K_{I_Z}\frac{T_s z}{z-1} + K_{D_Z}\frac{z-1}{T_s z}, \quad I_{HFC\ ref}(z) = C_{I_{HFC}}(z)e_Z(z), \tag{5}$$

where $K_{P_Z} = 245.3276$ A/m, $K_{I_Z} = 3.831$ kA/(m×s), $K_{D_Z} = 0.366$ (A×s)/m. The output $I_{HFC\ ref}$ of the controller, is limited to the range ±2 kA.

The Anti-Windup approach [13] was implemented during the synthesis of the controller to prevent saturation of the controller's output signal and the subsequent internal instability in the control system. In both controllers, a clamping mechanism is used, whereby integration is stopped when the signal at the controller output is outside the set range, and the output and input of the integrator have the same sign.

Figure 5 shows the results of controller synthesis using the method from [11], including the specified shaping functions and singular values of the discrete transfer functions of the synthesized system with models for the time points [3.229; 3.299; 3.449] s from shot model no. 5121 and [2.479; 2.489; 2.5] s from shot model no. 5126.

The open-loop transfer function array is given by

$$L_n(z) = G_n(z)C_Z(z), \quad Z(z) = L_n(z)e_Z(z), \tag{6}$$

where $G_n(z)$ is the array of inner loop transfer functions from (4), and $C_Z(z)$ is the transfer function of the controller (5). The sensitivity function array is given by

$$S_n(z) = \Big(I + L_n(z)\Big)^{-1}, \quad e_Z(z) = S_n(z)Z_{ref}(z),$$

the array of complementary sensitivity functions is

$$T_n(z) = L_n(z)S_n(z), \quad Z(z) = S_n(z)Z_{ref}(z),$$

the array of static and low-frequency sensitivity functions is

$$F_n(z) = \Big(G_n(1)K_{I_Z}T_s\Big)^{-1}(z-1), \text{ for small } \omega, \ z = \exp(j\omega T_s),$$

the array of Q-parameters is

$$Q_n(z) = C_Z(z)S_n(z), \quad I_{HFC\ ref}(z) = Q_n(z)Z_{ref}(z)$$

and the array of transfer functions from external input disturbance to $e_Z(z)$ is

$$W_n(z) = -S_n(z)G_n(z).$$

The specified shaping functions b_S and b_T limit the arrays of transfer functions $S_n(z)$ and $T_n(z)$ over the entire frequency range, ensuring the required robustness and quality margins for the closed-loop control system.

4. ROBUST STABILITY ANALYSIS OF THE PLASMA POSITION CONTROL CASCADE

To calculate the robust stability margins of the closed-loop system, the open-loop transfer function array (6) was used. Figure 6 shows the gain margins, and Fig. 7 shows the delay margins.

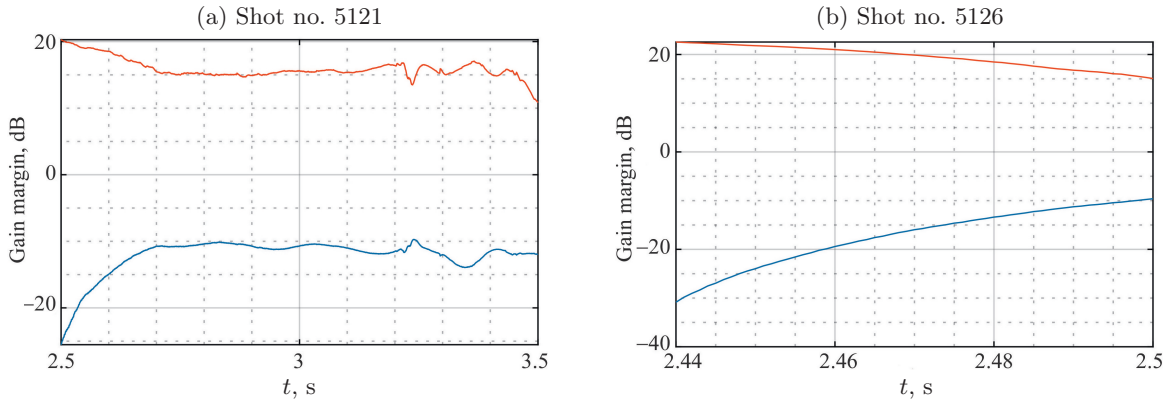

Fig. 6. Gain margin of the linear closed-loop control system.

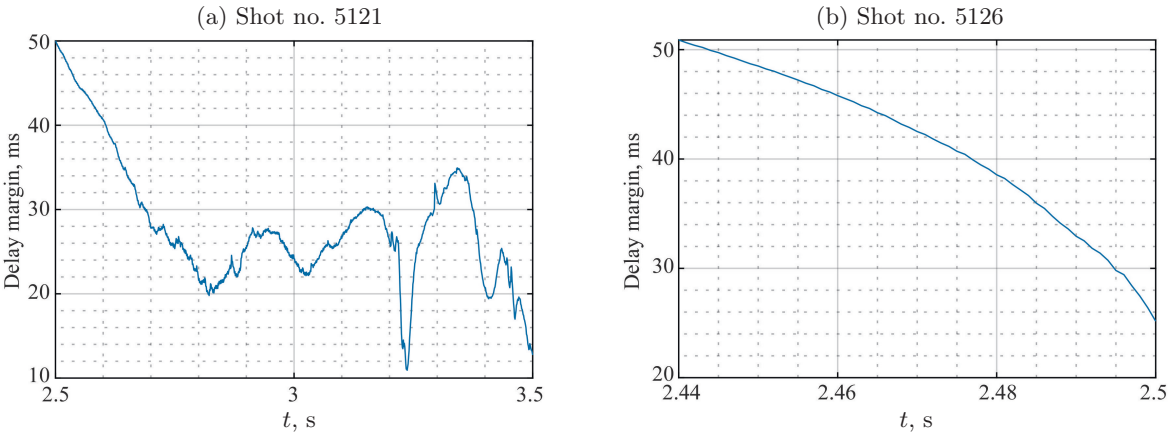

Fig. 7. Delay margin of the linear closed-loop control system.

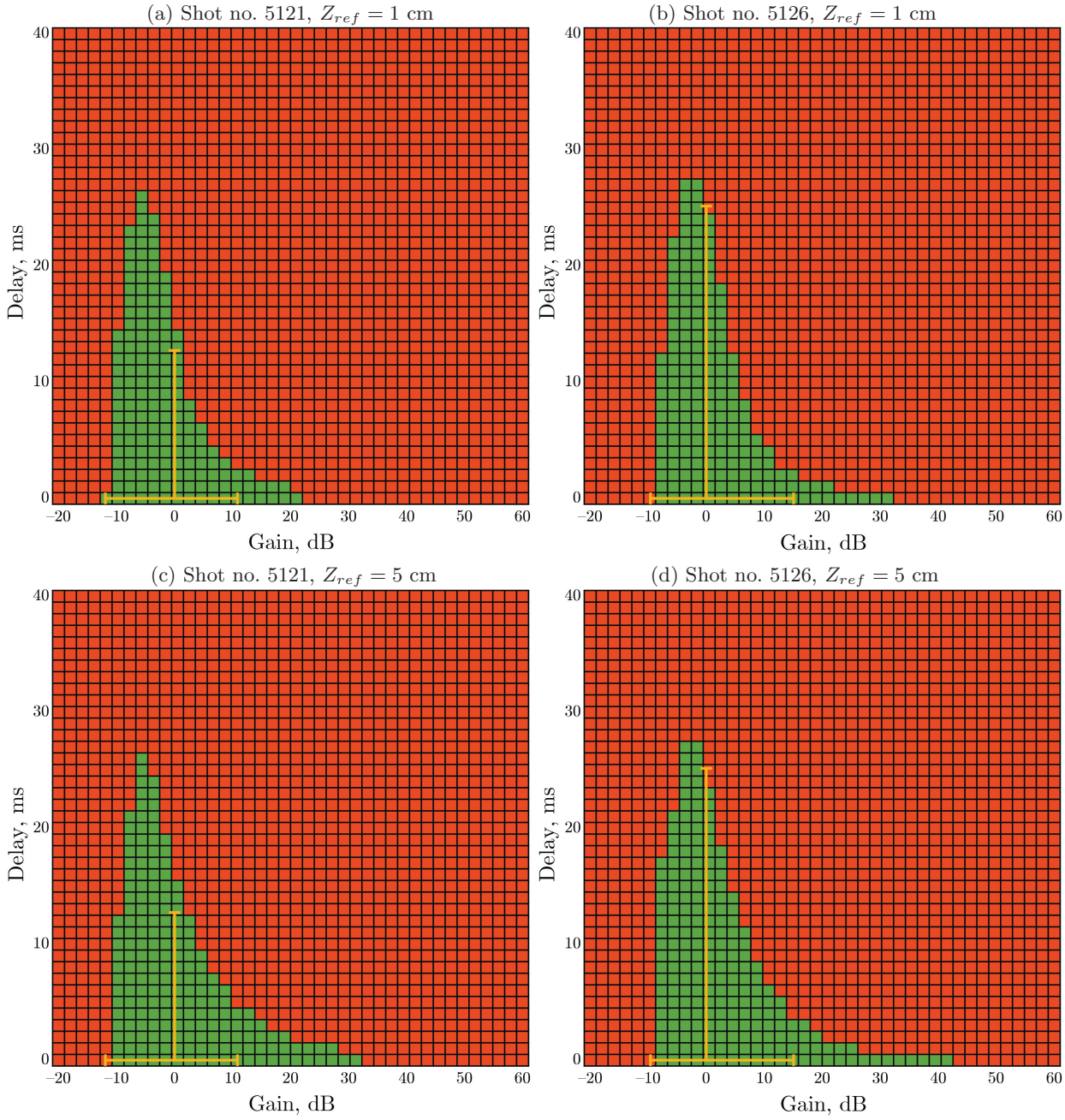

Fig. 8. Robust stability diagram of the nonlinear control system.

The delay margin T_M was calculated using the formula [14]:

$$T_M = \frac{\phi_M}{\omega_c}\frac{\pi}{180^\circ},$$

where ϕ_M is the phase margin, and ω_c is the gain crossover frequency (the frequency at which the open-loop gain first reaches the value 1). In the worst-case scenario, which occurs at the end of both shots, the synthesized control system has a satisfactory gain margin of ±10 dB (Fig. 6). The delay margin (Fig. 7) also exceeds the required 10 ms throughout both shots.

Figure 8 shows the stability diagrams of the nonlinear control system with the full model of the voltage inverter and the plasma vertical displacement model with variable parameters.

The delay and gain in the plasma vertical position feedback loop were varied. The nonlinear system has a limited controllability region, so the larger the reference input Z_{ref}, the smaller its robustness margins. Green indicates situations where the system is asymptotically stable, red indicates instability, and yellow shows the robustness margins of the linear model in the worst-case scenario (Figs. 6 and 7).

5. HARDWARE-IN-THE-LOOP SIMULATION

Hardware-in-the-loop simulation of the digital control system was conducted on the real-time test bed [15] at the Trapeznikov Institute of Control Sciences of RAS on two real-time target machines (RTTM). The structural scheme of the control system for hardware-in-the-loop simulation is shown in Fig. 9.

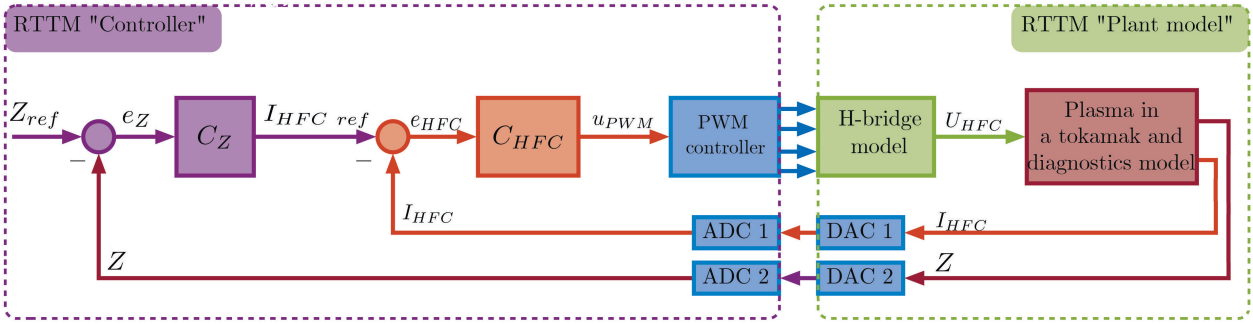

Fig. 9. Block diagram of the digital cascade control system for plasma vertical position in KTM during Hardware-in-the-loop simulation.

The digital controller is implemented on the RTTM "Controller," where, in addition to the controllers of both cascades, there is a PWM controller. This approach eliminates the need for using a DAC, which enhances the system's reliability and performance since the control signal u_{PWM} is not converted to analog. It is not necessary to spend time converting the signal to the DAC, also there is no need to ensure electromagnetic compatibility in the transmission line for the analog signal u_{PWM}, and the cost of implementing the PWM controller in analog form is reduced

On the RTTM "Plant model" is the model of vertical plasma displacement and the H-bridge model with a constant voltage source implemented in Simscape Electrical. The sampling time for the controllers is 1 ms, while the sampling time for the PWM controller, the H-bridge, and the vertical plasma displacement model is 100 μs. The sampling times differ by a factor of 10 to allow the PWM duty cycle to be 10%. If the control system implementation requires even smaller PWM duty cycle, the PWM controller can be implemented on an FPGA.

The concept of hardware-in-the-loop simulation of control systems assumes that part of the system is real, while the other part is represented by a model. In this case, all components of the controller are implemented on the RTTM "Controller." To make the controller functionally analogous to the one that will be used in the real control system (Fig. 2), there are two DACs at the output of the RTTM "Plant model."

5.1. Control System Simulation in Normal Operating Conditions

The results of hardware-in-the-loop simulation of the synthesized system in normal operating condition with a reference for the vertical plasma position of 5 cm are shown in Fig. 10. In addition to the transient process of the vertical plasma position and electrical signals from the power supply

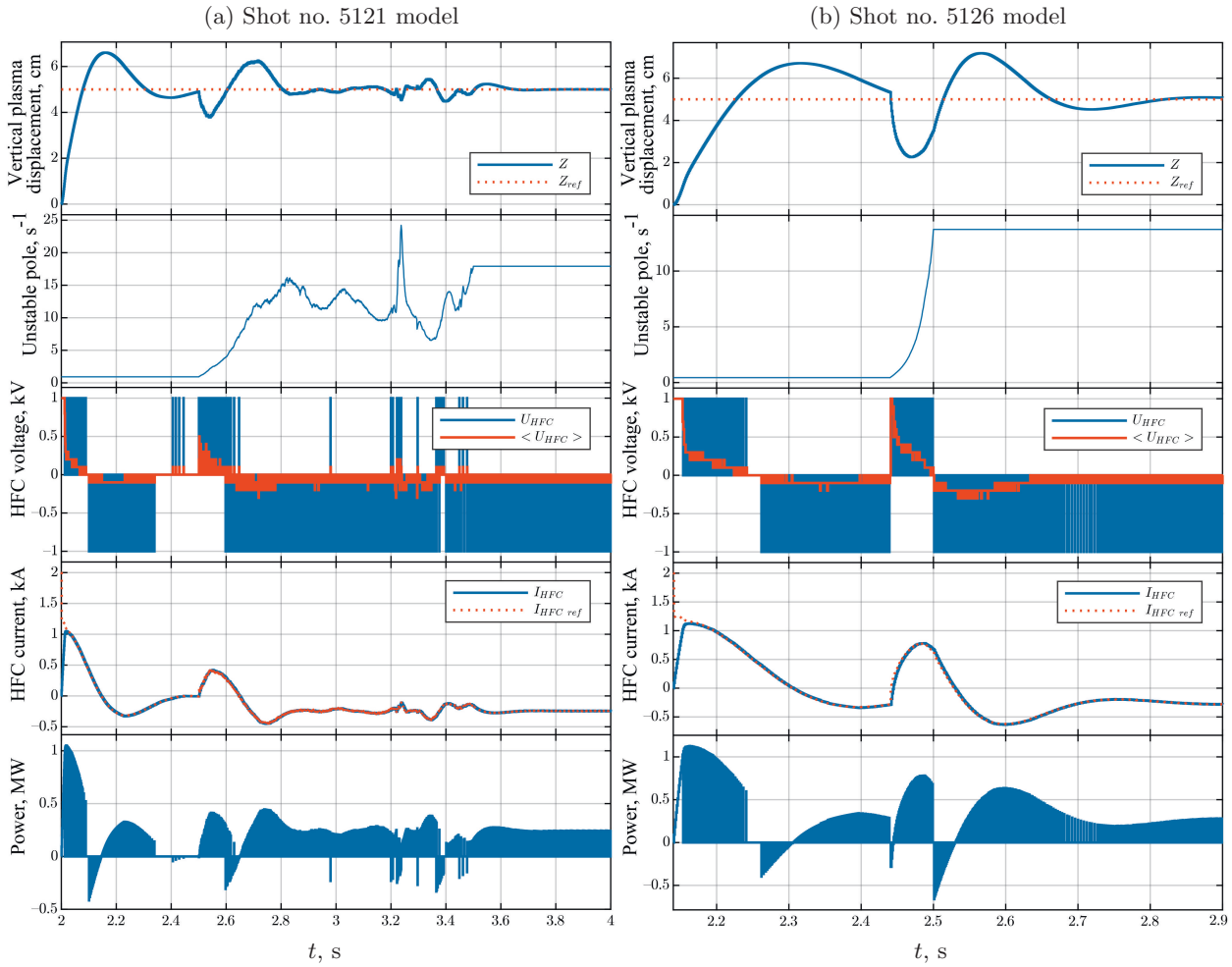

Fig. 10. Simulation of the plasma vertical position control system in KTM. The reference displacement is $Z_{ref} = 5$ cm.

(voltage, current, and power), the change in the unstable pole of the model for each shot is shown. The synthesized controller provides acceptable control quality for both vertical plasma displacement models. The required power of the voltage inverter does not exceed 1.2 MW, with a maximum possible power of 2 MW.

5.2. Control System Simulation in Extreme Operating Conditions

Figure 11 shows the results of hardware-in-the-loop simulation with the maximum vertical plasma displacement, at which the closed-loop system remains stable and provides acceptable control quality, and Fig. 12 shows the results for the maximum possible delay in the feedback loop for vertical plasma displacement. A plasma displacement of more than 10 cm vertically in the tokamak KTM is not required in practice, as this would cause the plasma separatrix to collide with the tokamak limiter. Therefore, the synthesized control system allows the control of vertical plasma position in the KTM tokamak over the entire possible range. In both cases, the delay exceeds the required 10 ms.

In [8], the upper bound of the vertical plasma position controllability region was calculated. For shot no. 5121 it is 23 cm, and for shot no. 5126 it is 26 cm. The actual controllability region for shot no. 5121 is 4 cm larger than the previously estimated value, which is explained by the fact

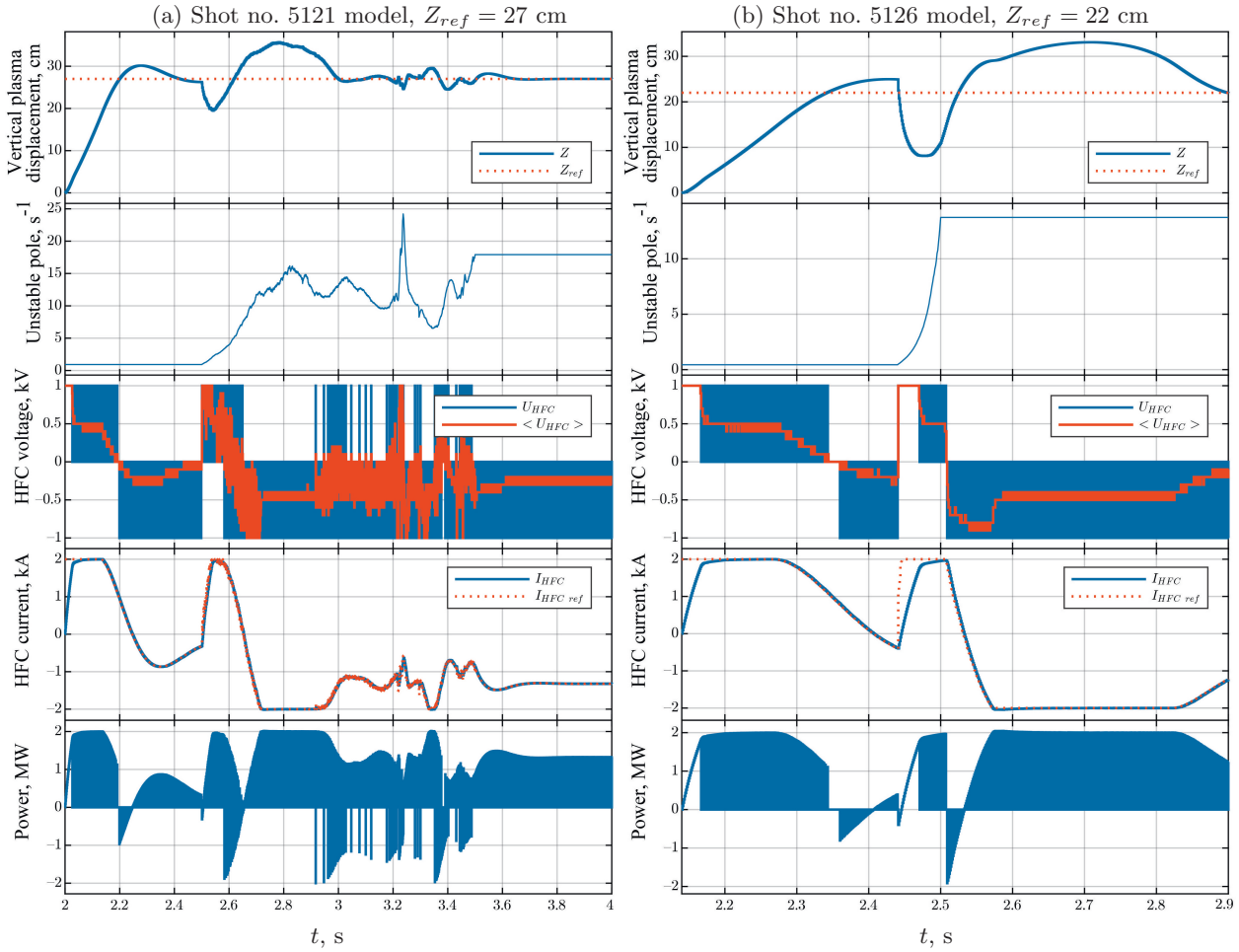

Fig. 11. Simulation of the plasma vertical position control system in KTM. The reference displacement is $Z_{ref} = 5$ cm.

that [8] used a model for one time point of the shot with the highest value of the unstable pole, which is not at the end of the shot, and any potential instability does not have time to develop. This also explains why the maximum delay of 14 ms (Fig. 12a) exceeds the minimum delay margin (Fig. 7a).

6. CONCLUSION

The operability of the control system has been demonstrated through hardware-in-the-loop simulation on two models of vertical plasma displacement, calculated based on experimental data from discharges with different scenarios. The full model of the voltage inverter in PWM mode, accounting for power limitations, was used in the simulation. With sufficient verification of the models used, the hardware-in-the-loop simulation guarantees the functionality of the control system when implemented in practical experiments.

The maximum possible vertical plasma displacement in the synthesized system with a voltage inverter in PWM mode is 27 cm for shot model no. 5121 and 22 cm for shot model no. 5126, which exceeds the actual required range of 10 cm. The maximum possible transport delay in the feedback loop for vertical plasma position, at which stability and acceptable control quality are maintained, is 14 ms for shot model no. 5121 and 23 ms for shot model no. 5126, which also exceeds the required value of 10 ms.

This work used a robust approach, where one controller is synthesized to meet the control quality and robust stability margin criteria simultaneously for multiple models of vertical plasma

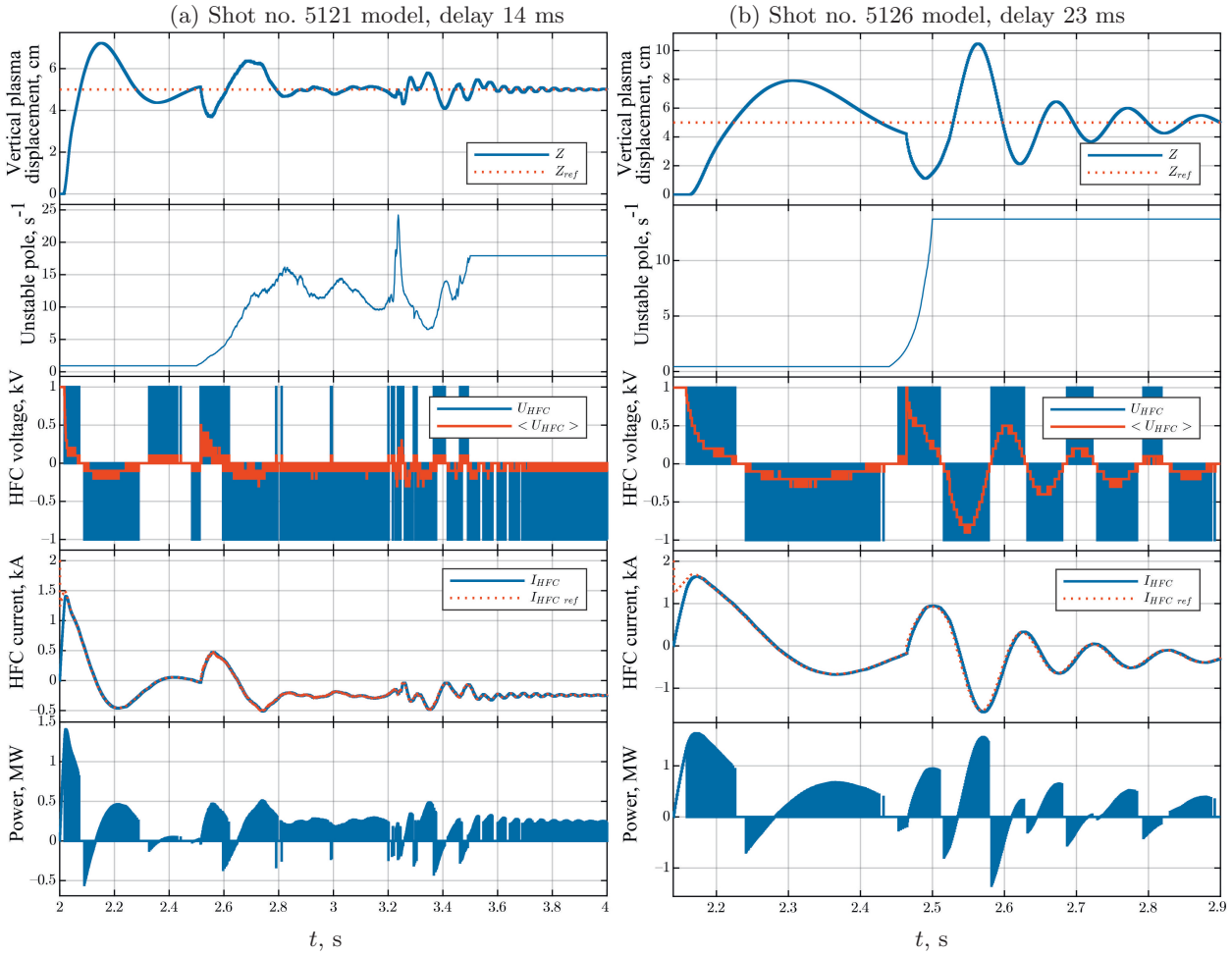

Fig. 12. Simulation of the plasma vertical position control system in KTM with the maximum possible delay in the feedback loop.

displacement. An alternative adaptive approach is possible, where the controller is tuned for a specific scenario or its parameters change during the discharge. The adaptive approach allows for better control quality since, in the case of the robust approach, the control quality is limited by the "worst-case" plant model. In this task, the robust approach is preferred over the adaptive one, as it does not require retuning the controller when the plasma discharge scenario changes.

FUNDING

This work was supported by the Russian Science Foundation project (no. 21-79-20180), as well as by the scientific and technical program IRN no. BR23891779 "Scientific-technical support of experimental research at the Kazakhstan material-testing KTM tokamak" under the program-targeted funding of the Ministry of Energy of the Republic of Kazakhstan.

APPENDIX

COMPARISON OF THE DIGITAL CONTROL SYSTEM WITH DISCRETIZED ANALOG CONTROL SYSTEM

The synthesis method [11] allows for the synthesis of both discrete and continuous control systems. A common approach is to apply a discretized controller in a digital control system. For example, in [16–19], continuous controllers were synthesized for plasma control in a tokamak. To demonstrate the drawbacks of this approach, the following comparison is made.

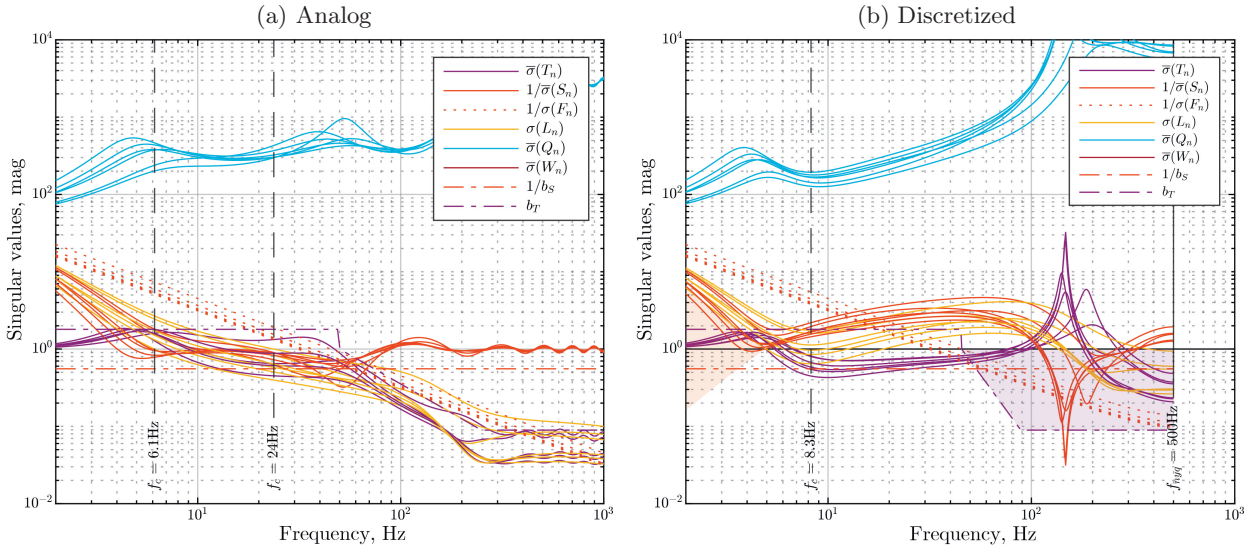

Fig. 13. Bode plot of the transfer functions of the analog and discretized plasma vertical position control system.

Figure 13a shows the result of synthesizing a continuous controller on the plant model in continuous time with the same shaping functions that were used for synthesizing the discrete controller in Section 3. The shaping functions in the synthesis method [11] define the control quality and the robustness margins of the closed-loop system, so the synthesized analog control system has approximately the same control quality and robustness margins as the digital system obtained earlier in Section 3.

The synthesized analog PID controller is given by the transfer function

$$\hat{C}_Z(s) = \hat{K}_{P_Z} + \hat{K}_{I_Z}\frac{1}{s} + \hat{K}_{D_Z}\frac{s}{\tau s + 1},$$

where $\hat{K}_{P_Z} = 266.9$ A/m, $\hat{K}_{I_Z} = 10.3$ kA/(m×s), $\hat{K}_{D_Z} = 0.53$ (A×s)/m, $\tau = 100$ μs, s – Laplace transform variable. After discretizing this controller using the ZOH method, the frequency response of the transfer functions of the discretized system was computed (Fig. 13b). The discretized control system is unstable.

In [20], it is shown that discretization may have little effect on the degradation of control quality and robustness margins, provided the closed-loop bandwidth is at least 30 times smaller than the sampling frequency. The closed-loop bandwidth of the control system varies depending on the shot time from 10 to 79 Hz, which means that the sampling time $T_s = 1$ ms is almost 2.5 times larger than needed to preserve control quality during discretization. Moreover, the plant model is not minimum-phase since it contains delay elements, which also contributes to the loss of stability of the control system during discretization.

REFERENCES

1. Mitrishkin, Y.V., Korenev, P.S., Prokhorov, A.A., et al., Plasma Control in Tokamaks. Part 1. Controlled thermonuclear fusion problem. Tokamaks. Components of control systems, *Advanc. Syst. Sci. Appl.*, 2018, vol. 18, no. 2, pp. 26–52.
2. Mitrishkin, Y.V., Kartsev, N.M., Pavlova, E.A., et al., Plasma Control in Tokamaks. Part 2. Magnetic plasma control systems, *Advanc. Syst. Sci. Appl.*, 2018, vol. 18, no. 3, pp. 39–78.
3. Mitrishkin, Y.V., Kartsev, N.M., Konkov, A.E., et al., Plasma Control in Tokamaks. Part 3.1. Plasma Magnetic Control Systems in ITER, *Advanc. Syst. Sci. Appl.*, 2020, vol. 20, no. 2, pp. 82–97.

4. Mitrishkin, Y.V., Kartsev, N.M., Konkov, A.E., et al., Plasma Control in Tokamaks. Part 3.2. Simulation and Realization of Plasma Control Systems in ITER and Constructions of DEMO, *Advanc. Syst. Sci. Appl.*, 2020, vol. 20, no. 3, pp. 136–152.

5. Ariola, M. and Pironti, A., *Magnetic Control of Tokamak Plasmas*, Springer International Publishing, 2016.

6. Korotkov, V.A., Azizov, E.A., Cherepnin, Yu.S., et al., Kazakhstan Tokamak for Material Testing Conceptual Design and Basic Parameters, *Fusion Engineering and Design*, 2001, vol. 56, pp. 831–835.

7. Zarva, D.B., Deriglazov, A.A., Batyrbekov, E.G., et al., Electrical Power Supply Complex of the Pulse Power System of the KTM Tokamak, *VANT. Ser. Termoyadernyi sintez*, 2018, vol. 41, no. 2, pp. 59–70.

8. Korenev, P.S., Konkov, A.E., Chektibaev, B.Zh., et al., Estimation of the Controllability Region of the Vertical Plasma Position in the KTM Tokamak with the HFC Coil, *VANT. Ser. Termoyadernyi sintez*, 2024, vol. 47, no. 3.

9. Mihalic, F., Truntic, M., and Hren, A., Hardware-in-the-Loop Simulations: A Historical Overview of Engineering Challenges, *Electronics*, 2022, vol. 11, p. 2462.

10. Batyrbekov, E.G., Tajibaeva, I.L., Baklanov, V.V., et al., Research in the field of controlled thermonuclear fusion in the Republic of Kazakhstan, *VANT. Ser. Termoyadernyi sintez*, 2024, vol. 47, no. 2, pp. 15–22.

11. Konkov, A.E. and Mitrishkin, Y.V., Synthesis Methodology for Discrete MIMO PID Controller with Loop Shaping on LTV Plant Model via Iterated LMI Restrictions, *Mathematics*, MDPI Publ., 2024, vol. 12, no. 6, p. 810.

12. Konkov, A.E. and Mitrishkin, Y.V., Comparison Study of Power Supplies in Real-Time Robust Control Systems of Vertical Plasma Position in Tokamak, *IFAC-PapersOnLine*, 2022, vol. 55, no. 9, pp. 327–332.

13. Grimm, G., Hatfield, J., Postlethwaite, I., et al., Antiwindup for stable linear systems with input saturation: An LMI-based synthesis, *IEEE Trans. Automat. Contr.*, 2003, vol. 48, no. 9, pp. 1509–1525.

14. Astrom, K. and Hagglund, T., *Advanced PID control*, ISA-The Instrumentation, Systems, and Automation Society, 2006.

15. Mitrishkin, Y.V., Konkov, A.E., and Korenev, P.S., Real-time Digital Simulation Testbed for Plasma Control in Tokamaks, *Materials of the XVI International Conference on Stability and Oscillations of Nonlinear Control Systems (Piatnitski Conference)*, 2022, pp. 286–289.

16. Mitrishkin, Y.V., Pavlova, E.A., Kuznetsov, E.A., and Gaydamaka, K.I., Continuous, Saturation, and Discontinuous Tokamak Plasma Vertical Position Control Systems, *Fusion Engineering and Design*, 2016, vol. 108, pp. 35–47.

17. Mitrishkin, Y.V., Prokhorov, A.A., Korenev, P.S., and Patrov, M.I., Hierarchical Robust Switching Control Method with the Improved Moving Filaments Equilibrium Reconstruction Code in the Feedback for Tokamak Plasma Shape, *Fusion Engineering and Design*, 2019, vol. 138, pp. 138–150.

18. Kruzhkov, V.I., Tuning of the Plasma Position Control System and Poloidal Currents in the Globus-M2 Tokamak and Its Implementation on the Real-Time Testbed, *Proceedings of the 17th All-Russian School-Conference of Young Scientists "Control of Large Systems"* (UBS'2021, Moscow), Moscow–Zvenigorod: Institute of Control Sciences named after V.A. Trapeznikov RAS, 2021, pp. 704–710.

19. Mitrishkin, Y.V., Korenev, P.S., Konkov, A.E., Kartsev, N.M., and Smirnov, I.S., New Horizontal and Vertical Field Coils with Optimised Location for Robust Decentralized Plasma Position Control in the IGNITOR Tokamak, *Fusion Engineering and Design*, 2022, vol. 174, p. 112993.

20. Franklin, G., Powell, J.D., and Workman, M.L., *Digital Control of Dynamic Systems*, Ellis-Kagle Press, 1997.

This paper was recommended for publication by N.N. Bakhtadze, a member of the Editorial Board